

79568-29-9; 1-Cl-*closo*-2,4-C₂B₅H₆, 79550-12-2; 3-Cl-*closo*-2,4-C₂B₅H₆, 79550-13-3; (CH₃)₃N-5-Cl-*closo*-2,4-C₂B₅H₆, 79534-17-1; [5-(CH₃)₃N-*closo*-2,4-C₂B₅H₆]⁺[BCl₄]⁻, 79534-19-3; [5-(CH₃)₃P-*closo*-2,4-C₂B₅H₆]⁺[BCl₄]⁻, 79534-21-7; [3-(CH₃)₃N-*closo*-2,4-

C₂B₅H₆]⁺[BCl₄]⁻, 79534-23-9; [5-(CH₃)₃N-6-CH₃-*closo*-2,4-C₂B₅H₅]⁺[BCl₄]⁻, 79550-15-5; [5-(CH₃)₃N-1-CH₃-*closo*-2,4-C₂B₅H₅]⁺[BCl₄]⁻, 79534-25-1; *closo*-2,4-C₂B₅H₇, 20693-69-0; (C-₃H₃)₃N, 75-50-3; NaBH₄, 16940-66-2.

Contribution from the School of Chemistry, University of Western Australia, Nedlands, Western Australia, Australia

A New Approach to the Structures and Rearrangements in *closo*-Boron Hydrides

D. J. FULLER and D. L. KEPERT*

Received May 13, 1981

A new approach to bonding in *closo*-boron hydrides, B_nH_n²⁻, has been developed in which each boron atom is considered to bond directly to all other boron atoms. A simple bireciprocal interaction is used to relate energy u to internuclear distance d : $u = 1/d^x - 1/d^y$. A good fit with experimental structures is found for low values of x and y , typical values being $x = 2$ and $y = 1$. This simple expression allows the assessment of a large number of complex molecular polyhedra in which the geometric parameters are allowed to vary freely in order to reach a minimum energy. For example, in B₁₂H₁₂²⁻ no less than 10 structures are found between the most stable stereochemistry, the regular icosahedron, and the cuboctahedron.

Two basic approaches have been used to describe the bonding in *closo*-boron hydrides, B_nH_n²⁻, and related compounds.¹ The first is a topological description of localized bonds. Each boron atom participates in four tetrahedrally arranged bonds, which may be B-H, B-B, or three-center B₃, the three boron atoms being in a triangular arrangement. A large number of resonance structures must be considered for any molecule. For example, each resonance form in the highly symmetrical structure of B₁₂H₁₂²⁻ has four different types of boron atoms, while in B₈H₈²⁻ all boron atoms must be different in any one resonance structure. One result from this approach to bonding is the prediction that the stable molecular polyhedra will be those that contain only triangular faces, but this may arise directly from the assumption of triangular three-center B₃ bonding.

The second approach is a molecular orbital treatment. Each boron atom uses one sp hybrid pointing out from the boron cluster for B-H bonding, the other pointing inward for bonding within the cluster. The single most bonding molecular orbital is that formed by the in-phase interaction of *all* these radial sp-hybrid orbitals at the center of the cluster, in an n -center bond that directly bonds each boron atom to every other boron atom. The two remaining p orbitals tangential to the surface of the cluster interact with similar orbitals on other boron atoms, and with the inwardly directed sp hybrids, to form very complicated molecular orbital schemes.

It is very difficult to use either of these approaches to accurately predict structural parameters such as bond lengths and bond angles or to assess the relative stability of the large number of transition states that can be visualized in intramolecular rearrangements.

In this work we explore an alternative bonding approach. Each boron atom is considered to interact simultaneously with *all* other boron atoms, the interactions depending *only* on the interatomic distances. A simple bireciprocal relation is used to describe the energy u_{ij} between two boron atoms i and j separated by a distance d_{ij} :

$$u_{ij} = \frac{1}{d^x} - \frac{1}{d^y} \quad \text{where } x > y$$

The total bonding energy is then

$$U = \sum_{ij} u_{ij}$$

where d and U are in arbitrary units. Values of x and y are obtained by fitting the resulting calculated structures against the known crystal structures of B₈H₈²⁻ and B₉H₉²⁻, which are the only simple compounds known with sufficient precision for this purpose. Some implications to the intramolecular rearrangements of B₈H₈²⁻, B₉H₉²⁻, and B₁₂H₁₂²⁻ are then discussed.

Structure of B₈H₈²⁻

The anion in [Zn(NH₃)₄][B₈H₈] is dodecahedral (Figure 1), with a crystallographic S₄ axis.² The four B_a atoms are 1.508 Å from the center of the cluster O, the O-B_a vectors making an angle of 31.1 ± 0.6° to the S₄ axis. The four B_b atoms are 1.315 Å from O, the O-B_b vectors making an angle of 105.7° to the same axis. The distance ratio (O-B_a)/(O-B_b) = 1.15 ± 0.02, which is intermediate between the dodecahedron constructed by making all boron-boron edge lengths equal, (O-B_a)/(O-B_b) = 1.374, and the dodecahedron formed by placing all boron atoms equidistant from the center.

Calculations based on the above energy expressions confirm that this dodecahedral structure is the only minimum on the potential energy surface, at all values of x and y . This is in contrast to eight-coordinate metal complexes where the square antiprism is the most stable structure,³ although the general forms of the potential energy surfaces are similar. The angular parameters are relatively insensitive to the values chosen for x and y , compared with the sharp dependence of the distance ratio, (O-B_a)/(O-B_b). The variation of (O-B_a)/(O-B_b) with x and y is shown in Figure 2, the shaded area corresponding to the value obtained from the crystal structure determination. A satisfactory fit between calculation and experiment is obtained, for example, for $x = 2.0$, $y = 1.0$, or $x = 1.5$, $y = 1.25$. Potentials of this type are very shallow and allow all boron-boron interactions to be significantly bonding.

Structure of B₉H₉²⁻

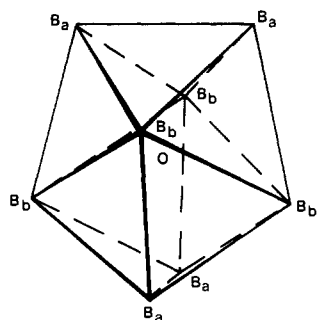
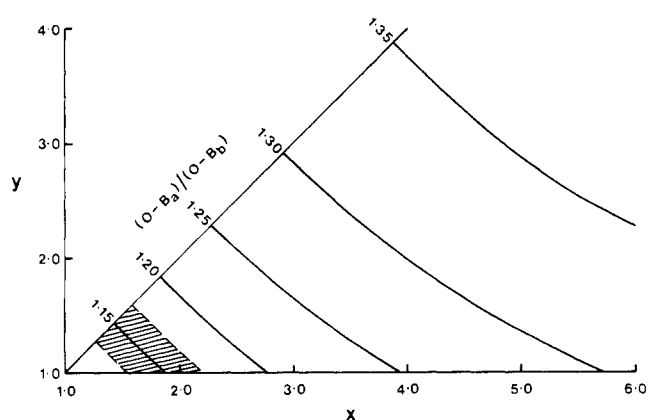
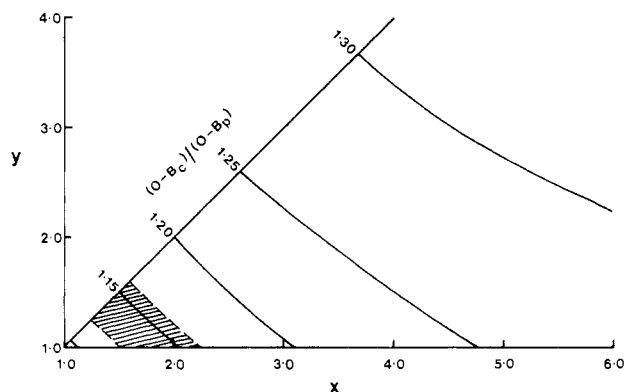
The structure of Rb₂[B₉H₉] is disordered, due to two different orientations of the tricapped trigonal-prismatic anion within the crystal.⁴ The ratio between the distance from the center of the cluster O to the capping atoms B_c and the distance between O and the prism atoms B_p is (O-B_c)/(O-B_p) = 1.14 ± 0.02. The angle six O-B_p vectors make to the threefold axis is 50.1 ± 1.0°. The distance ratio is again

(1) K. Wade, *Adv. Inorg. Chem. Radiochem.*, **18**, 1 (1976).

(2) L. J. Guggenberger, *Inorg. Chem.*, **8**, 2771 (1969).

(3) D. L. Kepert, *Prog. Inorg. Chem.*, **24**, 179 (1978).

(4) L. J. Guggenberger, *Inorg. Chem.*, **7**, 2260 (1968).

Figure 1. Structure of $B_8H_8^{2-}$.Figure 2. Variation of $(O-B_a)/(O-B_b)$ with x and y for $B_8H_8^{2-}$.Figure 3. Variation of $(O-B_c)/(O-B_p)$ with x and y for $B_9H_9^{2-}$.

intermediate between a polyhedron in which all B-B edge lengths are equal, $(O-B_c)/(O-B_p) = 1.304$, and a polyhedron in which all vertices are equidistant from the center.

Calculations based on the above energy expressions confirm that this tricapped trigonal-prismatic structure is the only minimum on the potential energy surface, at all values of x and y , which in this case is the same observation as for nine-coordinate metal complexes.⁵

The fit of the experimental parameter $(O-B_c)/(O-B_p)$ against the parameters calculated as a function of x and y is shown in Figure 3. The same values of x and y are obtained as were obtained for $B_8H_8^{2-}$; for example, $x = 2.0$, $y = 1.0$.

Alternatively it could have been claimed that the structure of $B_9H_9^{2-}$ can be reasonably accurately predicted with use of the values of x and y obtained for $B_8H_8^{2-}$.

Intramolecular Rearrangement of $B_8H_8^{2-}$

The $B_8H_8^{2-}$ ion is nonrigid in solution. The relative energies of possible transition states were calculated with use of the above birciprocal energy expression and $x = 2.0$, $y = 1.0$. All

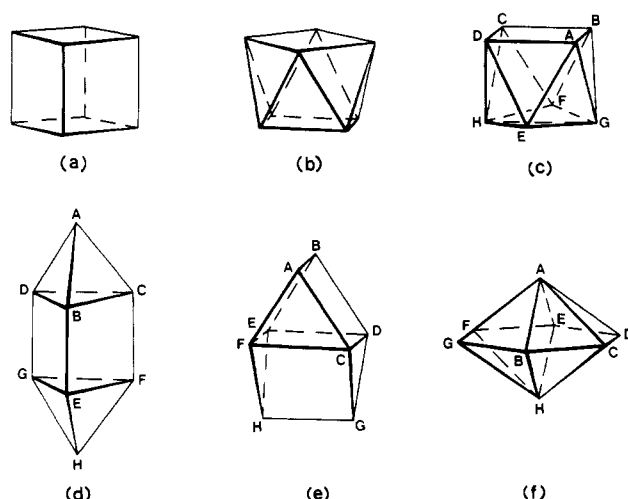


Figure 4. Polyhedra with eight vertices: (a) cube, (b) square antiprism, (c) bi(square-capped) trigonal prism, (d) bi(end-capped) trigonal prism, (e) gyrobifastigium, (f) hexagonal bipyramid.

Table I. Structural Parameters (Deg) for Eight-Atom Polyhedra^a

polyhedron	symmetry	atom	ϕ	θ	r
cube	O_h				1.469
square antiprism	D_{4d}		56.8	(0.0)	1.457
dodecahedron	D_{2d}	A	35.6	(0.0)	1.563
		B	107.4	(0.0)	1.351
bi(square-capped) trigonal prism	C_{2v}	A	54.8	45.7	1.494
		E	115.6	(0.0)	1.521
		G	126.6	(90.0)	1.325
bi(end-capped) trigonal prism	D_{3h}	A	(0.0)		2.073
		B	55.1	(0.0)	1.358
gyrobifastigium	D_{2d}	A	30.5	(0.0)	1.641
		C	(90.0)	(45.0)	1.320
hexagonal bipyramid	D_{6h}	A	(0.0)		1.102
		B	(90.0)	(0.0)	1.618

^a Values in parentheses are enforced by symmetry or by choice of axes.

polyhedra are shown in Figure 4, and the stereochemistries are defined with use of polar coordinates about the center of the polyhedron in Table I.

It is possible to construct six different convex polyhedra with eight vertices using regular polygons as faces. However, with the exception of the cube, all polyhedra that are calculated with use of the above energy expression are significantly distorted.

The cube is a regular polyhedron defined by r_A . For $x = 2$ and $y = 1$, the minimum energy is reached when $r_A = 1.469$.

The square antiprism is a semiregular polyhedron with two different types of faces, although all vertices remain identical. With use of $x = 2$ and $y = 1$, the polyhedron becomes elongated along the fourfold axis, reducing the size of the square faces at the expense of the triangular faces, so that $\phi_A = 56.8^\circ$, compared with $\phi_A = 59.3^\circ$ for a square antiprism based on squares and equilateral triangles.

The next five undistorted polyhedra are nonuniform. All have at least two kinds of vertices; that is, the boron atoms must be in geometrically different environments. The dodecahedron has been described above and is the observed structure for $B_8H_8^{2-}$. Two convex polyhedra can be formed by capping a trigonal prism, depending upon whether the square faces or the triangular faces are capped. Two triangular prisms sharing a square face form the gyrobifastigium. In these last three structures the polyhedra calculated for $x = 2$, $y = 1$ become significantly distorted by decreasing the size of the larger quadrilateral faces at the expense of the smaller triangular faces.

(5) M. C. Favas and D. L. Kepert, *Prog. Inorg. Chem.*, **28**, 309 (1981).

Table II. Bonding Energies for Eight-Atom Polyhedra

polyhedron	U	$U - U(\text{dodecahedron})$
dodecahedron	-6.7530	0.0000
bi(square-capped) trigonal prism	-6.7517	0.0013
square antiprism	-6.7512	0.0018
cube	-6.7189	0.0341
gyrobifastigium	-6.6944	0.0586
hexagonal bipyramid	-6.6804	0.0726
bi(end-capped) trigonal prism	-6.5900	0.1630

Table III. Structural Parameters (Deg) for Nine-Atom Polyhedra^a

polyhedron	symmetry	atom	ϕ	θ	r
tricapped trigonal prism	D_{3h}	A	46.6	(0.0)	1.423
		D	(90.0)	(60.0)	1.633
capped square antiprism	C_{4v}	A	(0.0)		1.568
		B	71.4	(0.0)	1.391
		F	130.6	(45.0)	1.581
capped cube	C_{4v}	A	(0.0)		1.652
		B	70.0	(0.0)	1.347
tridiminished icosahedron	C_{3v}	F	134.4	(0.0)	1.644
		A	40.0	(0.0)	1.508
		D	97.2	(0.0)	1.884
triangular cupola	C_{3v}	G	119.6	(60.0)	1.203
		A	40.2	(0.0)	1.532
		D	103.8	30.4	1.579

^a Values in parentheses are enforced by symmetry or by choice of axes.

Table IV. Bonding Energies for Nine-Atom Polyhedra

polyhedron	U	$U - U(\text{tricapped trigonal prism})$
tricapped trigonal prism	-8.6217	0.0000
capped square antiprism	-8.6195	0.0021
capped cube	-8.5679	0.0538
tridiminished icosahedron	-8.5013	0.1204
triangular cupola	-8.4479	0.1738

The remaining structure considered, the hexagonal bipyramid, cannot be constructed from equilateral triangles but is included for the sake of completion.

The total bonding energy, U , for each polyhedron is given in Table II. The same order is obtained for all values of x and y . More complete calculations of potential energy surfaces show that there are no potential energy barriers between these stereochemistries.

The order dodecahedron < bi(square-capped) trigonal prism < square antiprism is the same as that recently reported by Kleier and Lipscomb⁶ using the partial retention of diatomic differential overlap method. Considerably different results were obtained from extended Hückel theory⁷ and from MNDO calculations.⁸

Intramolecular Rearrangement of $B_9H_9^{2-}$

All nine-vertex polyhedra (Figure 5 and Table III) are nonuniform; that is, they must possess different types of vertices. Calculations using the above energy expression show that all polyhedra are distorted so that some faces are no longer regular polygons, the triangular faces increasing in size at the expense of the quadrilateral, pentagonal, and hexagonal faces.

The total bonding energy, U , for each polyhedron is given in Table IV, calculated for $x = 2$, $y = 1$. As the values of x and y increase, the order of stability among the three least stable polyhedra varies, but the three most stable polyhedra

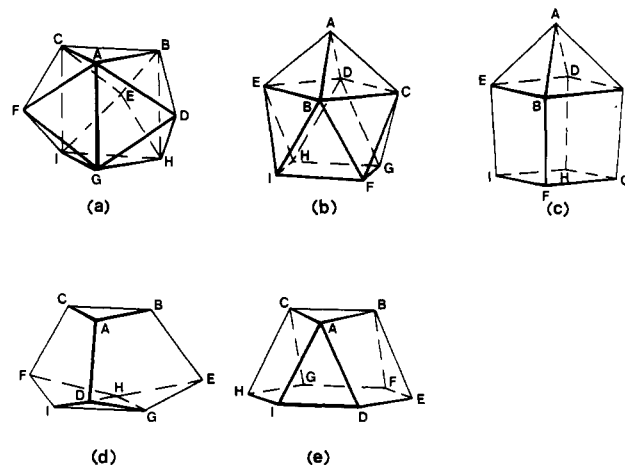


Figure 5. Polyhedra with nine vertices: (a) tricapped trigonal prism, (b) capped square antiprism, (c) capped cube, (d) tridiminished icosahedron, (e) triangular cupola.

Table V. Structural Parameters (Deg) for Twelve-Atom Polyhedra^a

polyhedron	symmetry	atom	ϕ	θ	r
regular icosahedron	I_h				1.586
cuboctahedron	O_h				1.601
truncated tetrahedron	T_d		30.9	(0.0)	1.696
hexagonal prism	D_{6h}		60.4	(0.0)	1.654
hexagonal antiprism	D_{6d}		61.1	(0.0)	1.653
bicapped pentagonal prism	D_{5h}	A	(0.0)		1.716
		B	61.1	(0.0)	1.574
square cupola	C_{4v}	A	38.0	(0.0)	1.750
		E	92.6	22.5	1.769
sphenomegacorona	C_{2v}	A	27.9	(0.0)	1.634
		C	75.3	57.1	1.484
		G	87.0	(0.0)	1.865
		I	127.7	(90.0)	1.770
		K	142.2	(0.0)	1.335
anticuboctahedron	D_{3h}	A	35.9	(0.0)	1.580
		D	(90.0)	31.8	1.618
D_{3h} icosahedron	D_{3h}	A	35.4	(0.0)	1.636
		D	(90.0)	(0.0)	1.872
		E	(90.0)	(60.0)	1.222
C_{3h} icosahedron	C_{3h}	A	35.4	6.2	1.638
		D	(90.0)	(0.0)	1.869
		E	(90.0)	61.4	1.220
		A	23.1	(0.0)	2.011
		C	60.9	58.9	1.878
tetracapped kite prism	C_{2v}	G	74.7	(0.0)	0.977
		I	113.4	(90.0)	1.394
		K	143.6	(0.0)	1.543
		A	43.9	44.5	1.600
		E	97.5	61.7	1.784
hebesphenocorona	C_{2v}	I	108.8	(0.0)	1.146
		K	151.9	(90.0)	1.666
		A	47.6	(0.0)	1.510
compressed cuboctahedron	D_{4h}	E	(90.0)	(45.0)	1.781
		A	42.5	(0.0)	1.736
elongated cuboctahedron	D_{4h}	E	(90.0)	(45.0)	1.319
		A	43.2	(0.0)	1.760
		E	(90.0)	44.7	1.560
orthorhombically distorted cuboctahedron	D_{2h}	F	(90.0)	134.7	0.922
		A	38.8	(0.0)	1.258
		C	70.3	62.8	1.788
disphenohedron	D_{2d}	A	38.8	(0.0)	1.258
		C	70.3	62.8	1.788

^a Values in parentheses are enforced by symmetry or by choice of axes.

remain tricapped trigonal prism < capped square antiprism < capped cube. Potential energy surfaces show that there are no barriers between these stereochemistries.

Structure and Intramolecular Rearrangement of $B_{12}H_{12}^{2-}$

The icosahedral structure of $B_{12}H_{12}^{2-}$ has been established for $K_2(B_{12}H_{12})$ ⁹ and $(Et_3NH)_2(B_{12}H_{12})$.¹⁰ The interest in

(6) D. A. Kleier and W. N. Lipscomb, *Inorg. Chem.*, **18**, 1312 (1979).

(7) F. Klanberg, D. R. Eaton, L. J. Guggenberger, and E. L. Muettterties, *Inorg. Chem.*, **6**, 1271 (1967).

(8) M. J. S. Dewar and M. L. McKee, *Inorg. Chem.*, **17**, 1569 (1978).

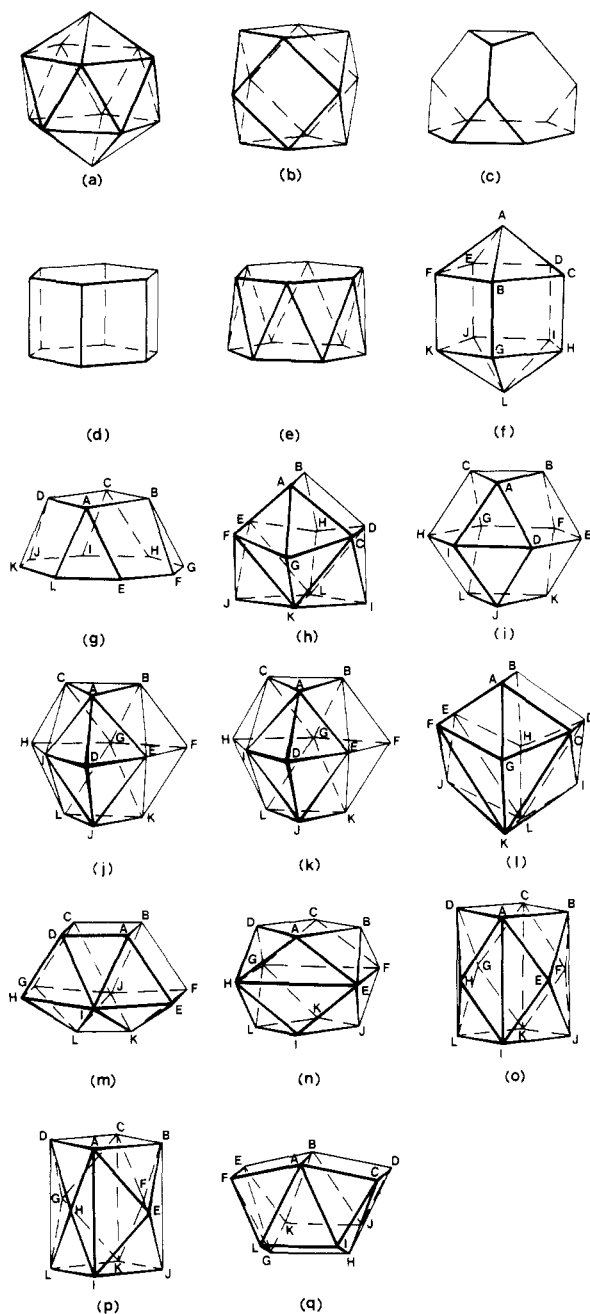


Figure 6. Polyhedra with twelve vertices: (a) regular icosahedron, (b) cuboctahedron, (c) truncated tetrahedron, (d) hexagonal prism, (e) hexagonal antiprism, (f) bicapped pentagonal prism, (g) square cupola, (h) sphenomegacorona, (i) anticuboctahedron, (j) D_{3h} icosahedron, (k) C_{3h} icosahedron, (l) tetracapped kite prism, (m) hebesphenocorona, (n) compressed cuboctahedron, (o) elongated cuboctahedron, (p) orthorhombically distorted cuboctahedron, (q) disphenohedron.

$B_{12}H_{12}^{2-}$ lies not only in the most stable stereochemistry but also in the intramolecular rearrangements of substituted carbaboranes.¹¹

The use of the above simple energy expression, with $x = 2$ and $y = 1$, allows the consideration of a large number of polyhedra (Figure 6 and Table V).

The icosahedron (Figure 6a) is a regular polyhedron with

- (9) J. A. Wunderlich and W. N. Lipscomb, *J. Am. Chem. Soc.*, **82**, 4427 (1960).
 (10) G. Shoham, D. Schomburg, and W. N. Lipscomb, *Cryst. Struct. Commun.*, **9**, 429 (1980).
 (11) H. D. Kaesz, R. Bau, H. A. Beall, and W. N. Lipscomb, *J. Am. Chem. Soc.*, **89**, 4218 (1967); H. V. Hart and W. N. Lipscomb, *ibid.*, **91**, 771 (1969); *Inorg. Chem.*, **12**, 2644 (1973).

all vertices identical, all edges equal, and all faces equilateral triangles.

The cuboctahedron (Figure 6b) is a semiregular polyhedron. All vertices are identical and all edges are identical, but now there are both equilateral triangular and square faces. The cuboctahedron is the transition state usually envisaged¹² when the rearrangements of icosahedral molecules are considered and allows transformations between the 1,2-carboranes and 1,7-carboranes. A center of symmetry is maintained during this transformation, and the cuboctahedron cannot lead to the 1,12-carboranes. Four threefold axes are maintained during this process, which can alternatively be pictured as simultaneous rotation of the triangular faces about the axes through their centers. The icosahedron and cuboctahedron are the only polyhedra for which the shape does not depend upon the values of x and y used in the potential function.

Four intersecting threefold axes are also present in the truncated tetrahedron (Figure 6c). This structure has also been postulated as an intermediate, and it may be noted that the structure of rhombahedral-105 boron can be viewed as being composed of either icosahedral (average B-B = 1.81 Å) or truncated tetrahedral (average B-B = 1.79 Å) units.¹³

Two additional semiregular polyhedra, which must be considered as they allow the twelve boron atoms to be geometrically equivalent, are the hexagonal prism (Figure 6d) and hexagonal antiprism (Figure 6e).

The next set of stereochemistries are derived from the nonuniform polyhedra, which are again constructed with use of regular polygons as faces, but now contain different types of vertices, that is, boron atoms in different environments. The bicapped pentagonal prism (Figure 6f) has been considered as a possible intermediate and is readily obtained by rotating half of an icosahedron relative to the bottom half by 36°. The apical atoms are 9% further away from the center of the molecule than are the prism atoms.

Three other structures derived from nonuniform polyhedra, the square cupola, the sphenomegacorona, and the anticuboctahedron, are defined in Figure 6g-i, respectively. If a body-centered cuboctahedron is considered as a remnant of cubic close packing, then a body-centered anticuboctahedron is a remnant of hexagonal close packing.

The next four structures are not derived from classical polyhedra composed of regular polygons. All are grossly distorted from the situation where all atoms lie on the surface of a sphere ($r = 0.922-2.011$), and some of the dihedral angles between adjacent faces are close to 180°. The D_{3h} icosahedron (Figure 6j) may be formed by rotating one face of a regular icosahedron, with large changes in the radial coordinates. Decreasing the applied symmetry from D_{3h} to C_{3h} by removal of the three twofold axes allows the ABCJKL prism to rotate slightly relative to the DEFGHI hexagon, leading to a more stable structure (Figure 6k). Further lowering of the applied symmetry to only C_3 by removal of the mirror plane while retaining $\theta_j = \theta_A$ does not result in any further stereochemical change.

The tetracapped kite prism (Figure 6l) and the hebesphenocorona (Figure 6m) have two and three quadrilateral faces, respectively.

During the course of these calculations it was found that additional stereochemistries could be generated simply by removing some of the imposed symmetry elements from the cuboctahedron, with retention of only two of the square faces (Figure 6n-p).

A number of other possible atom arrangements have been considered, but are not listed here as all were found to be less

- (12) A. Kaczmarczyk, R. D. Dobrott, and W. N. Lipscomb, *Proc. Natl. Acad. Sci. USA*, **48**, 729 (1962).
 (13) J. Donohue, "The Structures of the Elements", Wiley, New York, 1974.

Table VI. Bonding Energies for Twelve-Atom Polyhedra

polyhedron	U	$U - U(\text{icosahedron})$
icosahedron	-15.495 01	0.000 00
C_{3h} icosahedron	-15.436 35	0.058 66
D_{3h} icosahedron	-15.436 30	0.058 71
bicapped pentagonal prism	-15.431 11	0.063 90
tetracapped kite prism	-15.427 22	0.067 79
sphenomegacorona	-15.425 70	0.069 31
orthorhombically distorted cuboctahedron	-15.417 97	0.077 04
anticuboctahedron	-15.417 85	0.077 16
hebesphenocorona	-15.416 14	0.078 87
elongated cuboctahedron	-15.415 14	0.079 87
compressed cuboctahedron	-15.410 80	0.084 21
cuboctahedron	-15.408 87	0.086 14
disphenohedron	-15.335 43	0.159 58
hexagonal antiprism	-15.154 12	0.340 89
hexagonal prism	-15.132 76	0.362 25
truncated tetrahedron	-14.905 95	0.589 06
square cupola	-14.786 72	0.708 29

stable than the cuboctahedron. For example, 13 additional arrangements of 12 atoms have been depicted by Ciani and Sirona.¹⁴ One example is based on two layers of square nets, which form the disphenohedron shown in Figure 6q.

The bonding energies of the 17 polyhedra defined in Table V are summarized in Table VI. The icosahedron is the most stable structure as expected and the energy gap to the next most stable polyhedron (0.059) is very much greater than was found for $B_8H_8^{2-}$ (0.002) or $B_9H_9^{2-}$ (0.001). It can be seen that the cuboctahedron is *not* the most likely transition state, there being ten lower energy structures, all of lower symmetry and all containing more than one type of boron atom. The two lowest energy transition states are the closely related C_{3h} and D_{3h} icosahedra obtained by rotating one face of a regular icosahedron by 60° , with gross changes in the radial coordinates of the boron atoms, $r = 1.220-1.872$, compared with $r = 1.586$ for the regular icosahedron.

Figure 7 shows a potential energy surface in which only a threefold axis was enforced. There is no potential energy barrier between the deep minima of the regular icosahedra and the C_{3h} icosahedra, which are located as saddles between the regular icosahedra. Also shown are the D_{3h} icosahedra and the cuboctahedra and anticuboctahedra, which exist as maxima on this surface. More complete potential energy surfaces show the absence of any barrier between a regular icosahedron and a bicapped pentagonal prism.

As the values of x and y in the repulsion law increase, the C_{3h} icosahedron and D_{3h} icosahedron approach a hexagonal close packed array, which becomes more stable than a regular icosahedron (Figure 8).

These calculations confirm that face rotation is important in the rearrangement of substituted carboranes, $C_2B_{10}H_{12}$,^{11,15} although a more detailed comparison between prediction and experiment is not possible at this stage since the substitution of carbon for boron affects the mechanism by preferentially labilizing the faces trans to the carbon atoms.

(14) G. Ciani and A. Sirona, *J. Organomet. Chem.*, **197**, 233 (1980).
 (15) E. L. Muetterties and W. N. Knoth, "Polyhedral Boranes", Marcel Dekker, New York, 1968; E. L. Muetterties, *J. Am. Chem. Soc.*, **91**, 1636 (1969).

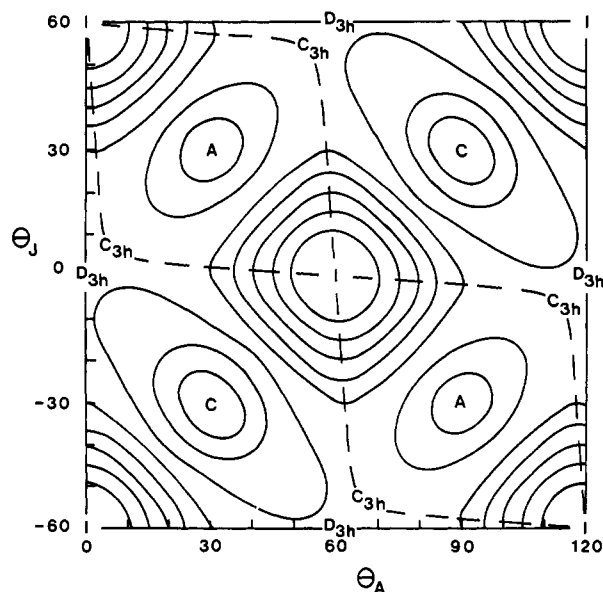


Figure 7. Projection of the potential energy surface for $B_{12}H_{12}^{2-}$ onto the $\theta_A-\theta_J$ plane (deg). The contour lines are for successive 0.01 increments above the minima at I; $x = 2, y = 1$. The position of the regular icosahedra (I), cuboctahedra (C), anticuboctahedra (A), D_{3h} icosahedra, and C_{3h} icosahedra are shown. The broken lines represent the reaction coordinates linking the regular icosahedra via the C_{3h} icosahedra.

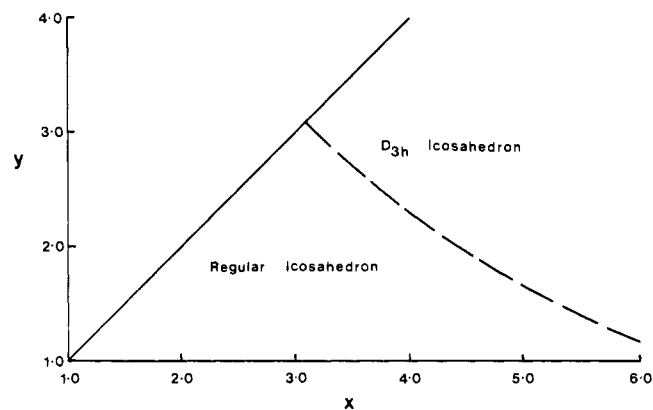


Figure 8. Most stable polyhedron for $B_{12}H_{12}^{2-}$ as a function of x and y .

Conclusion

This model is very simple and can readily be used to survey a wide range of structures in which the geometrical parameters are free to vary. The detailed geometry of any structure can therefore be easily predicted. The most stable structure is also easily determined and qualitative information obtained about the barriers to intramolecular rearrangements and possible transition states.

The model may be likened to metallic bonding, where each atom is bonded to all the surrounding atoms in spite of having only a few electrons available for bonding.

Registry No. $B_8H_8^{2-}$, 12430-13-6; $B_9H_9^{2-}$, 12430-24-9; $B_{12}H_{12}^{2-}$, 12356-13-7.